Strength and Ductility of High-Strength SFRC Confined by Spirals and Hoops Constructed with Self-Compacting Concrete

Nur Fithriani F. Cholida
Universitas Islam Sultan Agung, Indonesia | Civil Engineering Department, Universitas Semarang, Indonesia
nurfatma@usm.ac.id (corresponding author)

Antonius
Civil Engineering Department, Universitas Islam Sultan Agung, Indonesia
antonius@unissula.ac.id

Abdul Rochim
Civil Engineering Department, Universitas Islam Sultan Agung, Indonesia
abdulrochim@unissula.ac.id

Received: 11 December 2025 | Revised: 12 January 2026 and 30 January 2026 | Accepted: 11 February 2026

Licensed under a CC-BY 4.0 license | Copyright (c) by the authors | *DOI: https://doi.org/10.48084/etasr.16874*

ABSTRACT

This paper presents the results of an experimental investigation of high-strength Steel Fiber-Reinforced Concrete (SFRC) with Self-Compacting Concrete (SCC) containing spiral and hoop reinforcement, which was subjected to axial compressive loading. Forty cylindrical concrete specimens, each with a diameter of 100 mm and a height of 200 mm, were used to evaluate the effectiveness of producing confined SFRC using SCC by examining several design parameters, including the type of confining reinforcement (spiral and hoop), fiber volume fraction (0%, 0.5%, and 1%), as well as the spacing and yield strength of the confining reinforcement. The experimental results revealed that closer spacing of transverse reinforcement or a higher volumetric ratio enhances the strength of confined concrete (K) and increases ductility, as measured by the Toughness Index (TI). An increase in fiber volume fraction in confined concrete reduces the value of K; however, the TI increases, particularly when the transverse reinforcement spacing equals the specimen diameter. Specimens with a water-to-cement ratio (w/c) of 0.34, reinforced with spiral confinement, achieved an optimum K value of 1.51 at a fiber volume fraction (v_f) of 0%. Nevertheless, the highest ductility was observed in specimens with spiral confinement and a v_f of 1%, giving a TI value of 0.84. For a w/c mix design of 0.55, the optimum K value was obtained with hoop reinforcement (K = 1.54). However, the optimum ductility occurred in specimens with spiral confinement and v_f = 1%, resulting in a TI value of 0.87. A linear regression analysis of the experimental data indicates that the confinement effectiveness is 3.0.

Keywords-Self Compacting Concrete (SCC); steel fiber; confinement; strength; ductility

I. INTRODUCTION

The workability of high-strength SFRC is generally lower than that of normal-strength SFRC [1], thereby requiring continuous compaction using mechanical vibrators to achieve the desired strength [2, 3]. In practical applications, such as high-rise building construction, structural detailing often requires a high execution rate, particularly during the concreting process. The primary equipment employed for compaction includes internal and external vibrators; however, these do not always guarantee fully dense concrete [4]. Additionally, specifications for earthquake-resistant reinforced concrete structural elements typically require high reinforcement ratios, including optimal longitudinal reinforcement, reduced stirrup spacing (i.e., confined concrete detailing), and closely spaced confining reinforcement [5]. When conventional concrete is used under such conditions, there is a risk that vibrators may be unable to reach certain regions, which can lead to voids or porosity. In areas requiring meticulous execution, such as beam-column joints, significant concrete pressure during casting is necessary to ensure that the fresh concrete fully penetrates all regions of the joint and prevents the formation of porous concrete [5, 6]. Advances in concrete technology have led to the adoption of SCC because it exhibits excellent flowability and passing ability without

mechanical compaction [7-10]. These characteristics offer several advantages, such as faster construction, vibration-free placement, improved surface quality, and a simplified casting process. Consequently, SCC shows great promise for future structural applications. SCC can be produced using chemical admixtures such as superplasticizers, Viscocrete, or SS-8 [6, 11]. Incorporating these admixtures facilitates the production of Steel Fiber-Reinforced (SFR)-SCC by adding steel fibers in specific proportions [12, 13]. Using SCC in concrete construction results in enhanced mechanical performance compared to conventional methods [14, 15]. This improvement is primarily attributed to changes in the behavior of confined SFRC, which can exhibit compressive strengths ranging from normal to high values [16, 17]. The presence of confining reinforcement significantly influences the strength and ductility of confined concrete. Consequently, SCC SFRC exhibits superior overall performance compared to non-SCC steel fiber concrete [18, 19]. Several design parameters governing the behavior of SCC SFRC require investigation. These include concrete compressive strength, confining reinforcement spacing, and the yield strength of the confining steel [20]. Authors in [17, 21] examined the behavior of confined SFRC, but their study was limited to non-SCC construction methods. Authors in [22, 23] focused on confined SFR-SCC specimens with square cross-sectional geometries. The present study experimentally examined the behavior of circular-section SFR-SCC under confinement. The circular section provides more uniform lateral confinement pressure in all directions, making it suitable for simulating confined concrete behavior. This study primarily aims to evaluate the behavior of SFRC by examining several design parameters, including w/c, fiber volume fraction (v_f), characteristics of the confining reinforcement (volumetric ratio, spacing, and yield stress), and the type of confining reinforcement (spiral and hoop).

II. EXPERIMENTAL PROGRAM

A. Materials

All constituent materials, including the mixing water, fine aggregates with maximum particle sizes of 5 mm, and coarse aggregates with a maximum nominal size of 19 mm, were purchased locally and proportioned to satisfy the required grading specifications. Ordinary Portland Cement (OPC) grade 53 was selected due to its widespread commercial availability. Class F fly ash, supplied by the Tanjung Jati Jepara Steam Power Plant, was used as a supplementary cementitious material. The straight steel fibers utilized had aspect ratios of 60–70, an average tensile strength of approximately 500 MPa, and a modulus of elasticity of 5,000 MPa, as shown in Figure 1.

B. Mix Design

Two concrete mix designs were used to prepare the test specimens, with w/c ratios of 0.34 and 0.55. Based on preliminary experiments, a Consol SS-8 type superplasticizer was incorporated into SFR-SCC at a dosage of 0.6% by weight of cement. The concrete mix proportions are detailed in Table I [24]. The steel fiber volume fraction (v_f) was varied to 0%, 0.5%, and 1% of the total concrete volume for each mix design.

Fig. 1. Image of cut steel fiber.

TABLE I. CONCRETE MIX DESIGN

Materials	***w/c*=0.34**	***w/c*=0.55**
Cement (kg/m^3)	441	350
Fly ash (kg/m^3)	89	-
Water (lt/m^3)	152	192
Sand (kg/m^3)	697	723
Coarse aggregate (kg/m^3)	1045	887
Admixture type F (kg/m^3)	4.07	2.75

C. Specimens and Test Setup

The concrete specimens were cylindrical, measuring 100 mm in diameter and 200 mm in height. They were cast without a concrete cover to evaluate the behavior of purely confined concrete under passive confinement conditions. The yield strength (f_y) of the confining steel reinforcement, which consisted of spiral and hoop reinforcement, was determined through tensile testing, as depicted in Figure 2. To measure strain in the confining reinforcement, FLA-5-11 strain gauges were attached directly to the steel bars. All specimens were tested using a 1500 kN capacity compression testing machine equipped with a deformation-controlled loading system. Data obtained from the tests included the applied load and axial deformation, which were measured using Linear Variable Differential Transformers (LVDTs) installed in the axial direction. All data were continuously monitored and recorded using a data logger, and subsequently processed for further analysis.

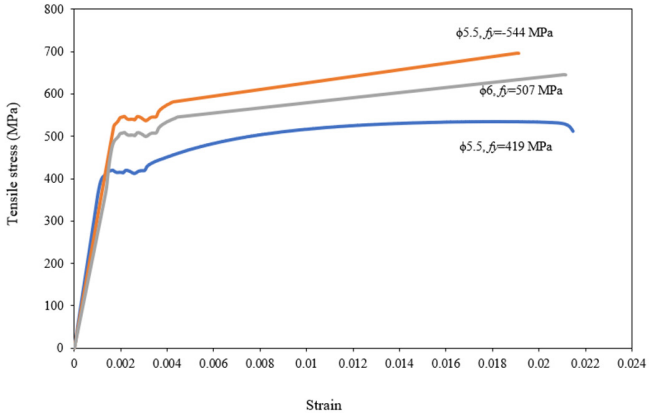

Fig. 2. Stress-strain curves of confining reinforcement.

The confined concrete stress (f_{ccf}) was calculated by dividing the applied load by the cross-sectional area of the specimen. The strength enhancement of confined concrete (K

value) is defined as the ratio of the confined concrete peak stress to 85% of the unconfined concrete cylinder strength (150 x 300 at 28 days) and is expressed as f_{ccf}' /(0.85 f_{ccf}'). The *K* value plays a significant role in determining the minimum volumetric ratio of confining reinforcement required in the design of reinforced concrete columns. Meanwhile, the confined concrete strain was calculated as the ratio of the axial deformation, as measured by LVDTs, to the specimen's original height. The ductility of confined concrete was evaluated using TI, determined by the methodology illustrated in Figure 3. In this study, the TI value was defined as the ratio of the shaded area under the stress-strain curve to the area bounded by ODEC.

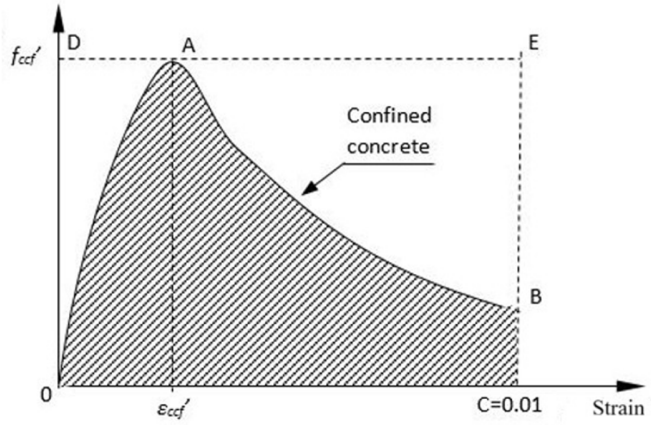

Fig. 3. Definition of TI.

III. RESULTS AND DISCUSSION

A. Results of Self-Compacting Concrete

Figure 4 shows the testing procedures for SCC conducted in accordance with ASTM C1611. The results of the slump flow test, L-box test, and V-funnel test are summarized in Table II [25]. These results indicate that the produced concrete satisfied the 2002 EFNARC requirements and can therefore be classified as SCC [26]. Subsequently, SFR-SCC was produced based on validated mix designs. Confinement testing of concrete specimens was conducted at a 35-day concrete curing age, along with the unconfined control tests, as portrayed in Figure 5.

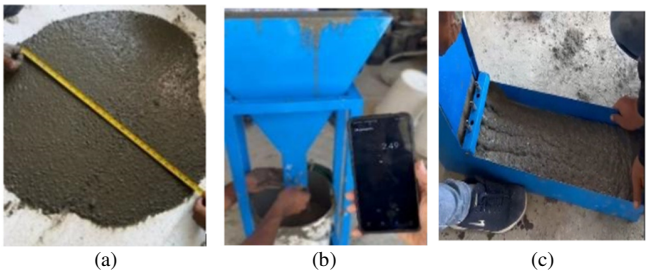

(a) (b) (c)

Fig. 4. SCC tests: (a) slump flow test, (b) V-funnel test, (c) L-box shape test.

The unit weight of the tested specimens ranged from 23.0 kN/m³ to 24.91 kN/m³. This range was observed across all specimens, which included different steel fiber volume fractions (v_f). The experimental program assumed that the density of SFR-SCC was comparable to that of conventional concrete. The measured values confirm that this assumption is reasonable. All cylinder testing procedures refer to ASTM C 39/C 39M – 01 [27]. Figure 5 demonstrates that specimen failure did not occur suddenly, which can be attributed to the installed confining reinforcement.

TABLE II. RESULTS OF SCC TESTING

Test method	Units	Acceptance criteria		Results
		Minimum	Maximum	
Slump flow	mm	650	800	670
L-shape box	H2/H1	0.8	1.0	0.82
V-funnel	sec	6	12	7.38

Fig. 5. Testing of confined concrete.

B. Confinement Behavior

The experimental results for SFR-SCC are summarized in Table III. After 28 days, the compressive strength of SFRC (f_{cf}'), with a w/c ratio of 0.34, increased from 50.3 MPa at v_f = 0% to 58.8 MPa at v_f = 0.5%, and then to 65.2 MPa at v_f = 1%. For specimens with a w/c ratio of 0.55, the compressive strength was 40.6 MPa at v_f = 0.5% and increased to 47.6 MPa at v_f = 1%. These results demonstrate a correlation between an increased steel fiber volume fraction and enhanced SCC compressive strength. The stress-strain behavior of confined concrete is expressed by the relationship between the strength enhancement factor (*K*) and confined concrete strain (axial strain).

1) Influence of Spiral and Hoop Spacing

The spacing of the confining reinforcement directly affects the volumetric ratio of confinement, on the *K* and TI values, which were measured by comparing specimens with closer spacing (s = 50 mm) to those with s = 100 mm. Specimens with s = 50 mm correspond to a volumetric ratio of 2.4%, while specimens with s = 100 mm exhibit a volumetric ratio of 1.2%. The w/c, steel fiber volume fraction (v_f), and yield strength of the confining reinforcement (f_y) were constant in all comparisons. The specimen pairs that were compared included

CS1 versus CS2, CS5 versus CS6, CS9 versus CS10, CH1 versus CH2, CH5 versus CH6, and CH9 versus CH10; all of these pairs corresponded to a v_f of 0.34. As displayed in Table III, specimens with closer spacing of the confining reinforcement consistently exhibited higher K and TI values. For instance, CS1 achieved K and TI values of 1.51 and 0.58, respectively, which are higher than those of CS2 (K = 1.20 and TI = 0.57). Similarly, CS5 (K = 1.35, TI = 0.69) outperformed CS6 (K = 1.14, TI = 0.55), and CS9 (K = 1.28, TI = 0.84) outperformed CS10 (K = 1.05, TI = 0.78). A similar trend was observed for specimens with a w/c ratio of 0.55. Those with 50 mm confining reinforcement spacing (CS13, CS17, CH13, and CH17) exhibited superior performance compared to those with 100 mm spacing (CS14, CS18, CH14, and CH18). Specifically, the specimens CS13 (K = 1.44, TI = 0.42), CS17 (K = 1.42, TI = 0.69), CH13 (K = 1.53, TI = 0.73), and CH17 (K = 1.46, TI = 0.60) demonstrated higher confinement effectiveness than the specimens CS14 (K = 1.12, TI = 0.53), CS18 (K = 1.04, TI = 0.66), CH14 (K = 1.21, TI = 0.62), and CH18 (K = 1.25, TI = 0.68). These results suggest that closer confinement reinforcement spacing increases lateral confining stress and enhances confinement effectiveness in the concrete core compared to specimens with wider spacing. The stress-strain responses of the confined concrete specimens presented in Figures 6 and 7 further confirm these observations. Specimens with tighter confining reinforcement spacing exhibited higher K values and a more ductile post-peak response, indicating enhanced confinement performance.

TABLE III. EXPERIMENTAL RESULTS

Specimen	w/c	v_f (%)	Confinement				f_{cf}' (MPa)	ε_{cf}'	f_{ccf}' (MPa)	K	TI
			Ø-spacing	ρ_{sh}	f_y (MPa)	Type					
CS1	0.34	0	6-50	0.024	507	Spiral	50.3	0.002	64.59	1.51	0.58
CS2			6-100	0.012	507			0.0022	51.31	1.20	0.57
CS3			5.5-50	0.02	419			0.0025	59.51	1.39	0.65
CS4			5.5-50	0.02	544			0.002	60.98	1.43	0.63
CH1			6-50	0.024	507	Hoop		0.0035	55.27	1.29	0.67
CH2			6-100	0.012	507			0.0029	54.39	1.27	0.52
CH3			5.5-50	0.02	419			0.003	58.3	1.36	0.64
CH4			5.5-50	0.02	544			0.0028	63.45	1.48	0.64
CS5	0.34	0.5	6-50	0.024	507	Spiral	58.8	0.0024	67.31	1.35	0.69
CS6			6-100	0.012	507			0.0024	56.78	1.14	0.55
CS7			5.5-50	0.02	419			0.0023	62.21	1.24	0.52
CS8			5.5-50	0.02	544			0.0024	65.22	1.30	0.47
CH5			6-50	0.024	507	Hoop		0.0025	65.96	1.32	0.69
CH6			6-100	0.012	507			0.0025	55.97	1.12	0.56
CH7			5.5-50	0.02	419			0.0018	65.37	1.31	0.7
CH8			5.5-50	0.02	544			0.0024	68.4	1.37	0.59
CS9	0.34	1	6-50	0.024	507	Spiral	65.2	0.0022	70.77	1.28	0.84
CS10			6-100	0.012	507			0.0022	58.09	1.05	0.78
CS11			5.5-50	0.02	419			0.0023	68.08	1.23	0.55
CS12			5.5-50	0.02	544			0.0021	71.29	1.29	0.55
CH9			6-50	0.024	507	Hoop		0.0023	67.69	1.22	0.64
CH10			6-100	0.012	507			0.0022	61.59	1.11	0.59
CH11			5.5-50	0.02	419			0.0023	70.78	1.28	0.54
CH12			5.5-50	0.02	544			0.0024	72.1	1.30	0.57
CS13	0.55	0.5	6-50	0.024	507	Spiral	40.6	0.0021	49.84	1.44	0.42
CS14			6-100	0.012	507			0.002	38.65	1.12	0.53
CS15			5.5-50	0.02	419			0.0022	48.11	1.39	0.62
CS16			5.5-50	0.02	544			0.0023	48.4	1.40	0.5
CH13			6-50	0.024	507	Hoop		0.0022	53.01	1.54	0.73
CH14			6-100	0.012	507			0.0018	41.76	1.21	0.62
CH15			5.5-50	0.02	419			0.0029	49.64	1.44	0.74
CH16			5.5-50	0.02	544			0.0027	51.07	1.48	0.68
CS17	0.55	1	6-50	0.024	507	Spiral	47.6	0.0028	57.28	1.42	0.69
CS18			6-100	0.012	507			0.0024	42.22	1.04	0.66
CS19			5.5-50	0.02	419			0.0025	53.57	1.32	0.69
CS20			5.5-50	0.02	544			0.0029	54.82	1.35	0.75
CH17			6-50	0.024	507	Hoop		0.0026	59.06	1.46	0.6
CH18			6-100	0.012	507			0.0024	50.73	1.25	0.68
CH19			5.5-50	0.02	419			0.0031	54.95	1.36	0.67
CH20			5.5-50	0.02	544			0.0037	55.88	1.38	0.87

2) Influence of Volume Fraction (v_f)

Figures 8 and 9 depict the stress-strain behavior of confined high-strength SFRC (w/c = 0.34) for specimens that were reinforced with hoops and spirals, respectively. To examine the influence of the steel fiber volume fraction (v_f), comparisons were made between specimens with identical volumetric ratios, reinforcement spacing, and yield strength of the confining reinforcement, while v_f was varied to 0%, 0.5%, and 1%.

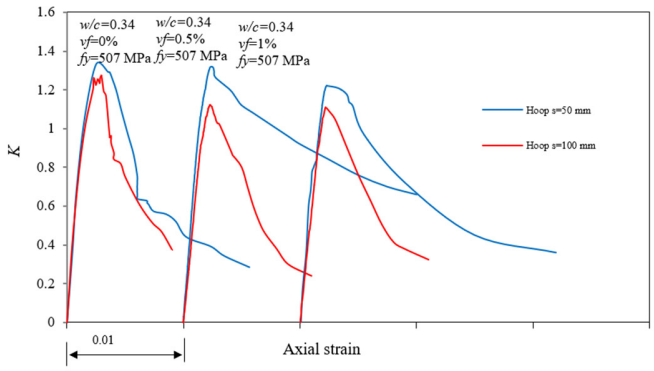

Fig. 6. Effect of hoop spacing.

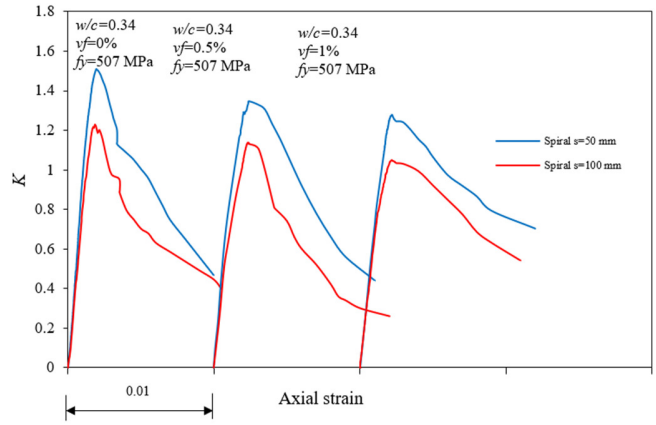

Fig. 7. Effect of spiral spacing.

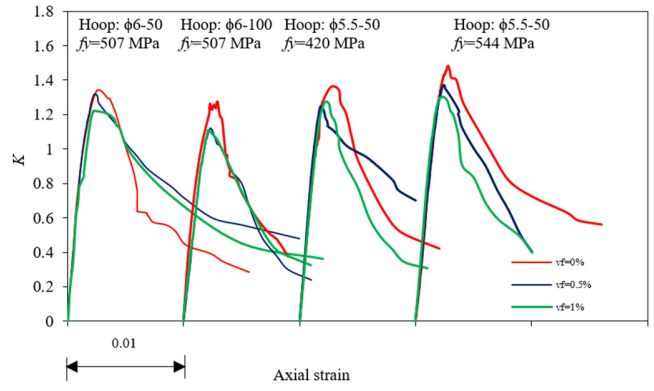

Fig. 8. Effect of v_f, specimens confined by hoops.

The optimal K and TI values for specimens with a hoop spacing of 50 mm and a yield strength of 507 MPa (CH1, CH5, and CH9) were achieved with a v_f of 0.5%. The corresponding K and TI values for these specimens were 1.29 and 0.67, 1.32 and 0.69, and 1.22 and 0.64, respectively. For specimens with a hoop spacing of 100 mm or a hoop volumetric ratio (ρ_h) of 1.2% (CH2 versus CH6 versus CH10), increasing v_f from 0% to 0.5% or 1% resulted in consistent decreases in K values and corresponding increases in TI values. This behavior indicates that, when the hoop spacing is equal to the specimen diameter, the mobilization of steel fibers enhances ductility in confined concrete, despite reducing confinement effectiveness (K value). A similar behavior was observed for specimens with hoops spaced 50 mm apart and f_y = 420 MPa (CH3 versus CH7 versus CH11), where increasing v_f resulted in decreasing K values while achieving the optimum TI at v_f = 0.5%. The corresponding K and TI values were 1.36 and 0.61, 1.31 and 0.70, and 1.28 and 0.54, respectively. In contrast, for specimens confined with 50 mm spacing and f_y = 544 MPa (CH4, CH8, and CH12), both K and TI values decreased consistently with increasing v_f. The respective K and TI values were 1.48 and 0.64, 1.37 and 0.59, and 1.30 and 0.57. The optimal K and TI values for specimens with a hoop spacing of 50 mm and a yield strength of 507 MPa (CH1 versus CH5 versus CH9) were achieved with a 0.5% volume fraction of voids. The corresponding K and TI values for these specimens were 1.29 and 0.67, 1.32 and 0.69, and 1.22 and 0.64, respectively. The performance of specimens confined with spiral reinforcement under identical spacing, volumetric ratio, and yield strength conditions, was evaluated. Specimen CS1 (v_f = 0%) exhibited K = 1.51 and TI = 0.58; specimen CS5 (v_f = 0.5%) showed K = 1.35 and TI = 0.69; and specimen CS9 (v_f = 1%) achieved K = 1.28 and TI = 0.84. These results suggest that the optimal K value occurs at v_f = 0.5%, while the optimal TI value occurs at v_f = 1%. Similarly, comparisons among specimens CS2 (K = 1.20, TI = 0.57), CS6 (K = 1.15, TI = 0.55), and CS10 (K = 1.05, TI = 0.78) revealed a behavior analogous to that of hoop-confined specimens. Increasing v_f resulted in a consistent reduction in K and an enhancement in TI. The highest ductility was observed at v_f = %. A different phenomenon was observed for specimens with identical spiral spacing and a yield strength of 50 mm and 420 MPa (CS3, CS7, and CS11). The corresponding K and TI values were 1.39 and 0.65, 1.24 and 0.52, and 1.23 and 0.55, respectively. These results suggest that specimens without steel fibers (v_f = 0%) achieved the optimum K and TI values, indicating that, under these conditions, the spiral confinement mechanism was more dominant than the contribution of steel fibers. A similar trend was observed for specimens CS4, CS8, and CS12 (spiral spacing = 50 mm; yield strength = 544 MPa), for which the respective K and TI values were 1.43 and 0.63, 1.30 and 0.47, and 1.29 and 0.55.

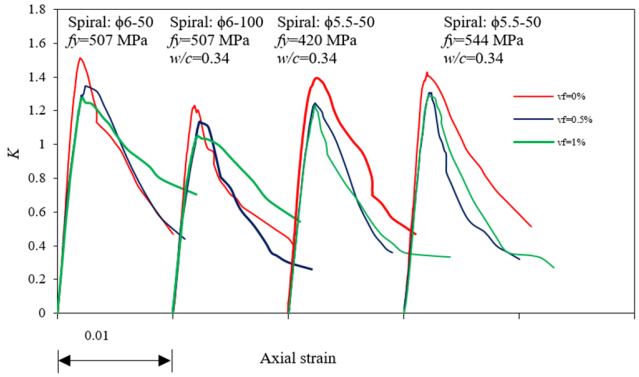

Fig. 9. Effects of v_f, specimens confined by spirals.

Based on these observations, increases in the fiber volume fraction (v_f) do not consistently result in higher values of the confinement effectiveness coefficient (K) or TI. This suggests

that the relationship between these parameters is not strictly proportional. The characteristics of the confining reinforcement, particularly the spacing and yield strength, also significantly impact the resulting confinement performance.

3) Effect of Yield Stress (f_y)

Figures 10 and 11 show the influence of the yield strength of the confining reinforcement on the stress-strain behavior of confined, high-strength, SFRC. Figures 10 and 11 compare specimens CH3 and CH4, CH7 and CH8, CH11 and CH12, CS3 and CS4, CS7 and CS8, and CS11 and CS12, with identical confinement spacing and volumetric ratios but with different yield strengths of the confining reinforcement (f_y = 419 MPa and 544 MPa). The stress-strain response shows that specimens confined with reinforcement of a higher yield strength had better K values. However, differences in post-peak behavior between specimens were generally minimal. Specimens confined with reinforcement of a lower yield strength (f_y = 419 MPa), such as CH3 (K = 1.36, TI = 0.64), CH7 (K = 1.31, TI = 0.70), CH11 (K = 1.28, TI = 0.54), CS3 (K = 1.39, TI = 0.65), CS7 (K = 1.24, TI = 0.52), and CS11 (K = 1.23, TI = 0.55), exhibited lower K and TI values than specimens confined with reinforcement of a higher yield strength (f_y = 544 MPa), such as CH4 (K = 1.48, TI = 0.64), CH8 (K = 1.37, TI = 0.59), CH12 (K = 1.30, TI = 0.57), CS4 (K= 1.43, TI = 0.63), and CS8 (K = 1.30, TI = 0.47), CS12 (K= 1.29, TI = 0.55). These findings suggest that using confining reinforcement with a higher yield strength—either hoop or spiral—for specimens with identical confinement spacing and volumetric ratios leads to enhanced confinement effectiveness and ductility.

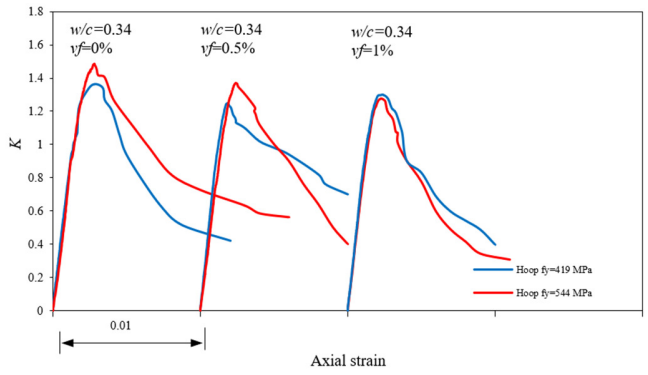

Fig. 10. Effect of yield stress of hoops.

4) Influence of The Type of Confinement

For normal concrete specimens (v_f = 0%), specimen CH1 exhibited a K value of 1.29 and a TI value of 0.67. These values were then compared to those of specimen CS1 (K value = 1.51 and TI value = 0.58). These comparisons were made under identical confinement spacing, volumetric ratio, and yield strength of the confining reinforcement. The results indicate that spiral confinement enhances confinement effectiveness (K value) more than hoop confinement, which provides greater ductility. In another comparison, with a confining reinforcement spacing equal to the specimen diameter and a yield strength of 507 MPa, specimen CH2 achieved a K value of 1.27 and a TI value of 0.52. Meanwhile, specimen CS2 exhibited a K value of 1.20 and a TI value of 0.57. In this case, hoop confinement was superior in terms of confinement effectiveness, while spiral confinement resulted in higher ductility. A further comparison of specimens CH3 (K = 1.36, TI = 0.64) and CS3 (K = 1.39, TI = 0.65), with constant volumetric ratio, spacing (ϕ5.5–50), and yield strength (f_y = 419 MPa), demonstrated that spiral confinement produced marginally higher K and TI values than hoop confinement. Conversely, for specimens CH4 and CS4, which were confined using reinforcement with a yield strength of 544 MPa, the resulting K and TI values were 1.48 and 0.64 for CH4 and 1.43 and 0.63 for CS4, respectively. These results suggest that under conditions of higher yield strength, hoop confinement outperforms spiral confinement in terms of confinement effectiveness and ductility.

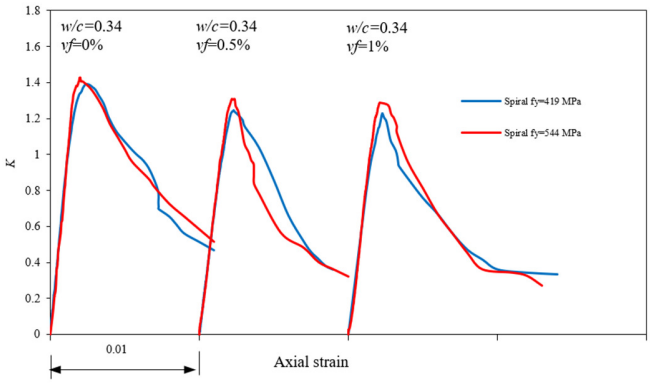

Fig. 11. Effect of yield stress of spirals.

The comparative performance of spiral and hoop confinement for high-strength, confined, SFRC with v_f = 0.5%, was evaluated. Specimens CH5 (K = 1.32, TI = 0.69) and CS5 (K = 1.35, TI = 0.69) were compared. Both were confined using ϕ6–50 reinforcement with f_y = 507 MPa. Spiral confinement produced a slightly higher K value, and both confinement types exhibited identical ductility. Similarly, a comparison of specimens CH6 (K = 1.12, TI = 0.56) and CS6 (K = 1.14, TI = 0.55), which used identical confinement reinforcement (ϕ6–100, f_y = 507 MPa), revealed negligible differences in K and TI values between spiral and hoop confinement. However, a different trend was observed for specimens CH7 (K = 1.31, TI = 0.70) and CS7 (K = 1.24, TI = 0.52), which were confined using reinforcement with a lower yield strength (f_y = 419 MPa). In this case, hoop confinement demonstrated superior performance to spiral confinement in terms of confinement effectiveness and ductility. Similar behavior was observed in the comparison between specimens CH8 and CS8, which used reinforcement with a higher yield strength (f_y = 544 MPa). Specimen CH8, confined with hoops, exhibited K = 1.37 and TI = 0.59, which were significantly higher than those of specimen CS8, which was confined with spirals (K = 1.30 and TI = 0.47). The performance of spiral and hoop confinement for specimens containing a 1% steel fiber volume fraction, was also evaluated. Specimens confined using ϕ6–50 reinforcement with f_y = 507 MPa revealed that spiral confinement continued to outperform hoop confinement. This

was evident in specimens CH9 (K = 1.22, TI = 0.64) and CS9 (K = 1.28, TI = 0.84). However, when the confinement spacing was doubled to ϕ6–100 with a yield strength of 507 MPa, the hoop-confined specimens exhibited slightly higher K values than the spiral-confined specimens. Nevertheless, spiral confinement resulted in greater ductility. This behavior is evident in the comparison of specimens CH10 (K = 1.11, TI = 0.59) and CS10 (K = 1.05, TI = 0.78). Furthermore, specimens CH11 and CS11 exhibited K values of 1.28 and 1.23, respectively, indicating that hoop confinement provided slightly higher confinement effectiveness. Nevertheless, the TI values of both specimens were comparable (0.54 and 0.55, respectively). Similar to the behavior observed in specimens with v_f = 0% and 0.5%, specimens containing 1% steel fibers and confined using reinforcement with the highest yield strength (ϕ5.5–50, f_y = 554 MPa) demonstrated superior performance with hoop confinement, such as specimens CH12 (K = 1.30, TI = 0.57) and CS12 (K = 1.29, TI = 0.55). Figures 12-14 illustrate comparisons of the stress-strain behavior of confined, high-strength, SFRC specimens using spiral and hoop confinement.

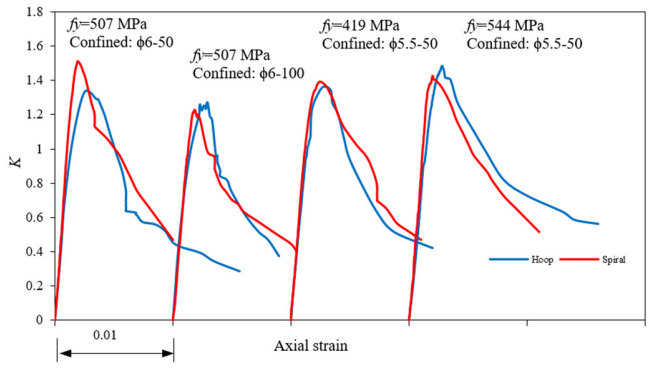

Fig. 12. Effect of confinement types, w/c=0.34, v_f=0%.

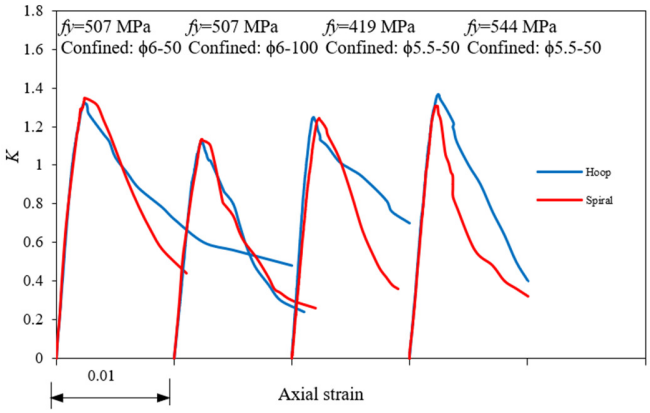

Fig. 13. Effect of confinement types, w/c=0.34, v_f=0.5%.

For the mix design with w/c = 0.34, specimens CS1 (v_f = 0%) and CS9 (v_f = 1%) exhibited identical confining reinforcement characteristics: ϕ6–50 spacing, a volumetric ratio of ρ_s = 2.4%, and a yield strength of f_y = 507 MPa. However, specimen CS1 exhibited the highest confinement strength enhancement factor (K = 1.51). In contrast, specimen CS9 exhibited the best ductility performance, with a TI value of 0.84. For the mix design with w/c = 0.55, the highest K value (1.54) was obtained for specimen CS13 (v_f = 0.5%), with confining reinforcement characteristics of ϕ6–50 spacing, a volumetric ratio of ρ_h = 2.4%, and a yield strength of f_y = 507 MPa. Meanwhile, the highest ductility was observed in specimen CS20 (v_f = 1%), which had confining reinforcement with ϕ5.5–50 spacing, a volumetric ratio of ρ_s = 2.0%, and a yield strength of f_y = 544 MPa.

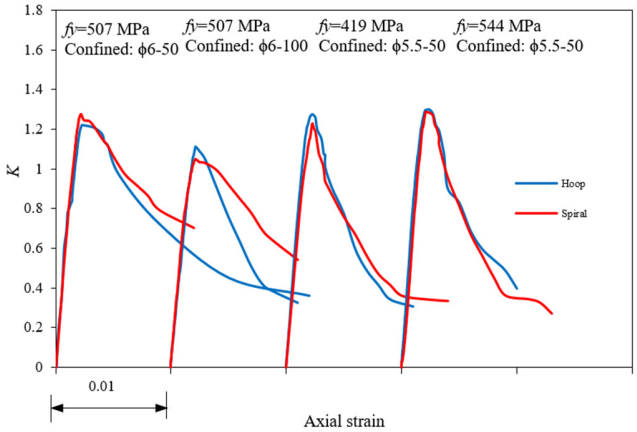

Fig. 14. Effect of confinement types, w/c=0.34, v_f=1%.

5) Strength Enhancement of Confined Concrete Based on Experimental Results

Figure 15 demonstrates the relationship between the confinement effectiveness factor (K) and the unconfined concrete compressive stress for all specimens listed in Table III. The lateral confining stress generated by the spiral and hoop reinforcements was calculated based on the equilibrium principle between the lateral confining force and the resisting force provided by the transverse reinforcement:

$$f_2 = \frac{2.A_s.f_y}{s.D} \quad (1)$$

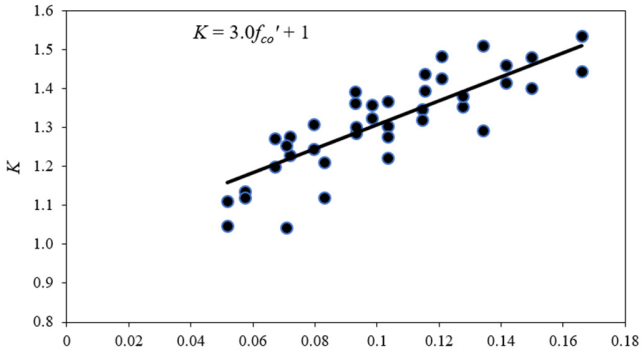

Fig. 15. A linier regression of K equation.

Linear regression analysis of the experimental data led to:

$$K = \frac{f_{cc}'}{f_{co}'} = 1 + 3.0\frac{f_2}{f_{co}'} \quad (2)$$

The results were compared to previously proposed expressions for the confinement effectiveness factor (K) for SFRC, as shown in Figure 16, presenting a linear relationship. However, a discrepancy was noted in the confinement effectiveness coefficient, which was measured at 3.0, lower than the value of 3.5, which was derived from triaxial compression tests representing active confinement conditions. The lower value obtained in this study can be attributed to the passive nature of the confinement provided by the spiral and hoop reinforcements in the reinforced concrete specimens. In contrast, authors in [28-30] proposed confinement models with nonlinear formulations to estimate K.

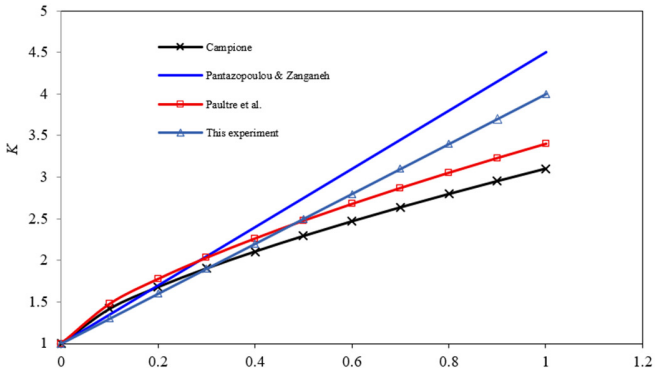

Fig. 16. Failure strength envelope of confined SFRC.

IV. CONCLUSIONS

Based on the experimental results obtained in this study, the following conclusions can be drawn:

- High-strength Steel Fiber-Reinforced Concrete (SFRC) can be produced using the Self-Compacting Concrete (SCC) method in accordance with the 2002 EFNARC requirements by incorporating an admixture (Consol SS-8) at a minimum dosage of 0.6% by weight of cement.
- The characteristics of the confining reinforcement significantly influence the K value and Toughness Index (TI). Closer spacing, a higher volumetric ratio of confining reinforcement, and higher yield strength lead to increased K values.
- The specimens with the same water-to-cement ratio (w/c) show that increasing the volume fraction of steel fibers reduces the confinement effectiveness factor (K) while increasing the TI. This indicates that steel fibers are more effective in enhancing the ductility of confined concrete than its peak compressive strength.
- In general, spiral reinforcement is more effective than hoop reinforcement at providing confinement, resulting in higher confinement strength factor (K) and ductility values. However, when high-yield-strength confining reinforcement (fy = 544 MPa) was used, hoop reinforcement outperformed spiral reinforcement in enhancing the mechanical performance of confined concrete.
- The predictive equation for the confinement effectiveness coefficient (K) proposed in this study, captures the key characteristics of the materials used and incorporates a confinement effectiveness coefficient of 3.0. This value is representative of Steel Fiber-Reinforced (SFR)-SCC under confinement, providing a realistic basis for application under conditions comparable to those commonly encountered in Indonesia.
- The present study is limited to SFRC-SCC specimens with circular cross sections. Further investigations are required to examine the effects of varying reinforcement configurations on confined SFRC in square sections.

ACKNOWLEDGMENT

The experimental program presented in this paper was funded by the Faculty of Engineering, Universitas Semarang (USM), Indonesia. The authors gratefully acknowledge the financial and technical support provided for the successful completion of this research.

NOTATIONS

ε_{cf}' peak strain of unconfined fiber-reinforced concrete

f_y yield strength of confining reinforcement

f_c' compressive strength of normal concrete (no fiber) of cylinder 150x300 mm at 28 days

f_{cf}' compressive strength of fiber concrete of cylinder 150x300 mm at 28 days

f_{ccf}' peak stress of confined steel fiber concrete

k confinement effectiveness

ϕ diameter of hoops or spirals

ρ_h volumetric ratio of hoop

ρ_s volumetric ratio of spiral

s spacing of confining reinforcement (center-to center)

v_f volume fraction of fiber

REFERENCES

[1] P. Smarzewski, "Mechanical properties and durability of ultra-high performance concrete containing steel fibers," *Composite Structures*, vol. 371, 2025, Art. no. 119471, https://doi.org/10.1016/j.compstruct.2025.119471.

[2] D. A. Karisma, A. I. Candra, M. K. K. Ali, T. S. Sari, and S. A. P. Pertiwi, "The optimum vibration of the compressive strength of concrete specimen," *INERSIA: Informasi dan Ekspose Hasil Riset Teknik Sipil dan Arsitektur*, vol. 18, no. 2, pp. 217–224, 2022, https://doi.org/10.21831/inersia.v18i2.54522.

[3] J. Gong, Y. Yu, R. Krishnamoorthy, and A. Roda, "Real-time tracking of concrete vibration effort for intelligent concrete consolidation," *Automation in Construction*, vol. 54, 2015, https://doi.org/10.1016/j.autcon.2015.03.017.

[4] *309-05: Guide for Consolidation of Concrete*. Farmington Hills, MI, USA: ACI, 2005.

[5] N. F. F. Cholida, A. Antonius, and F. Ni'am, "A parametric study of confinement effects to the interaction diagram of P–M for high-strength concrete columns," *Journal of Advanced Civil and Environmental Engineering*, vol. 1, no. 1, pp. 30–37, 2018, https://doi.org/10.30659/jacee.1.1.30-37.

[6] S. Y. Golla, K. Rajesh Kumar, M. I. Khan, Ch. Rahul, and K. Pruthvi Raj, "Structural performance of exterior beam-column joint using biochar impregnated pond ash concrete," *Materials Today: Proceedings*, vol. 39, pp. 467–471, 2021, https://doi.org/10.1016/j.matpr.2020.07.722.

[7] J. Karthik, H. J. Surendra, M. Anusha, and V. S. Prathibha, "Assessment of self-compacting concrete without superplasticizer in bridge construction," *Materials Today: Proceedings*, vol. 65, pp. 1558–1566, 2022, https://doi.org/10.1016/j.matpr.2022.04.516.

[8] P. Kumar, D. Pasla, and T. Jothi Saravanan, "Self-compacting lightweight aggregate concrete and its properties: A review," *Construction and Building Materials*, vol. 375, 2023, Art. no. 130861, https://doi.org/10.1016/j.conbuildmat.2023.130861.

[9] J. Wang, J. Zhou, and J. Kangwa, "Self-compacting concrete adopting recycled aggregates," in *Multi-Functional Concrete with Recycled Aggregates*, Elsevier, 2023, pp. 267–288, https://doi.org/10.1016/B978-0-323-89838-6.00007-4.

[10] M. A. Rashwan, T. M. Al Basiony, A. O. Mashaly, and M. M. Khalil, "Self-compacting concrete between workability performance and engineering properties using natural stone wastes," *Construction and Building Materials*, vol. 319, 2022, Art. no. 126132, https://doi.org/10.1016/j.conbuildmat.2021.126132.

[11] M. Deng, F. Ma, S. Song, H. Lü, and H. Sun, "Seismic performance of interior precast concrete beam-column connections with highly ductile fiber-reinforced concrete in the critical cast-in-place regions," *Engineering Structures*, vol. 210, 2020, Art. no. 110360, https://doi.org/10.1016/j.engstruct.2020.110360.

[12] S. G. Nehme, R. László, and A. El Mir, "Mechanical performance of steel fiber reinforced self-compacting concrete in panels," *Procedia Engineering*, vol. 196, pp. 90–96, 2017, https://doi.org/10.1016/j.proeng.2017.07.177.

[13] N. A. Memon, M. A. Memon, N. A. Lakho, F. A. Memon, M. A. Keerio, and A. N. Memon, "A Review on Self Compacting Concrete with Cementitious Materials and Fibers," *Engineering, Technology & Applied Science Research*, vol. 8, no. 3, pp. 2969–2974, June 2018, https://doi.org/10.48084/etasr.2006.

[14] B. Persson, "A comparison between mechanical properties of self-compacting concrete and the corresponding properties of normal concrete," *Cement and Concrete Research*, vol. 31, no. 2, pp. 193–198, 2001, https://doi.org/10.1016/S0008-8846(00)00497-X.

[15] K. K. Sideris and N. S. Anagnostopoulos, "Durability of normal strength self-compacting concretes and their impact on service life of reinforced concrete structures," *Construction and Building Materials*, vol. 41, 2013, https://doi.org/10.1016/j.conbuildmat.2012.12.042.

[16] Purwanto, Antonius, and L. Fitriyana, "Stress-strain response on the confined normal and high-strength concrete cylinders containing steel fiber under compression," *Advances in Concrete Construction*, vol. 17, no. 4, pp. 233–243, 2024, https://doi.org/10.12989/acc.2024.17.4.233

[17] A. Antonius, "Strength and energy absorption of high-strength steel fiber-concrete confined by circular hoops," *International Journal of Technology*, vol. 6, no. 2, pp. 217–224, 2015, https://doi.org/10.14716/ijtech.v6i2.860.

[18] D.L. Nguyen, D.K. Thai, N.T. Tran, T.T. Ngo, and H.V. Le, "Confined compressive behaviors of high-performance fiber-reinforced concrete and conventional concrete with size effect," *Construction and Building Materials*, vol. 336, 2022, Art. no. 127382, https://doi.org/10.1016/j.conbuildmat.2022.127382.

[19] B. Sabariman, A. Soehardjono, W. Wisnumurti, A. Wibowo, and T. Tavio, "Stress-strain behavior of steel fiber-reinforced concrete cylinders spirally confined with steel bars," *Advances in Civil Engineering*, vol. 2018, 2018, Art. no. 6940532, https://doi.org/10.1155/2018/6940532.

[20] H. G. Kim and K. H. Kim, "Effect of shape and amount of transverse reinforcement on lateral confinement of normal-strength concrete columns," *Advances in Concrete Construction*, vol. 14, no. 2, pp. 79–92, 2022, https://doi.org/10.12989/acc.2022.14.2.079.

[21] H. Aylie, Antonius, and A. W. Okiyarta, "Experimental study of steel-fiber reinforced concrete beams with confinement," *Procedia Engineering*, vol. 125, pp. 1030–1035, 2015, https://doi.org/10.1016/j.proeng.2015.11.158.

[22] X. Ni, B. Zhao, Y. Li, and Y. Hou, "Predicted compressive stress–strain model for high-strength stirrup confined concrete," *Structures*, vol. 52, pp. 933–945, 2023, https://doi.org/10.1016/j.istruc.2023.04.039.

[23] H. Aoude, W. D. Cook, and D. Mitchell, "Behavior of columns constructed with fibers and self-consolidating concrete," *ACI Structural Journal*, vol. 106, no. 3, 2009, https://doi.org/10.14359/56499.

[24] *7656:2012, Mix design techniques for normal concrete, heavyweight concrete, and mass concrete*. Indonesia: SNI, 2012.

[25] *C1611/C1611M-21 Standard Test Method for Slump Flow of Self-Consolidating Concrete*. West Conshohocken, PA, USA: ASTM International, 2021.

[26] *Specification and Guidelines for Self-Compacting Concrete*. Flums Hochwiese, Switzerland: EFNARC, 2002.

[27] *C39/C39M-21 Standard Test Method for Compressive Strength of Cylindrical Concrete Specimens*. West Conshohocken, PA, USA: ASTM International, 2023.

[28] S. J. Pantazopoulou and M. Zanganeh, "Triaxial Tests of Fiber-Reinforced Concrete," *Journal of Materials in Civil Engineering*, vol. 13, no. 5, pp. 340–348, Oct. 2001, https://doi.org/10.1061/(ASCE)0899-1561(2001)13:5(340).

[29] P. Paultre, R. Eid, Y. Langlois, and Y. Lévesque, "Behavior of Steel Fiber-Reinforced High-Strength Concrete Columns under Uniaxial Compression," *Journal of Structural Engineering*, vol. 136, no. 10, pp. 1225–1235, Oct. 2010, https://doi.org/10.1061/(ASCE)ST.1943-541X.0000211.

[30] G. Campione, "The effects of fibers on the confinement models for concrete columns," *Canadian Journal of Civil Engineering*, vol. 29, no. 5, pp. 742–750, Oct. 2002, https://doi.org/10.1139/l02-066.